

## MIRROR-CURVE CODES FOR KNOTS AND LINKS

Ljiljana Radović and Slavik Jablan

ABSTRACT. Inspired by Lomonaco–Kauffman paper on quantum knots and knot mosaics we construct the more concise representation of knot mosaics and grid diagrams via mirror-curves. We introduce codes for mirror-curves treated as knot or link diagrams placed in rectangular square grid, suitable for software implementations and discuss possible applications of mirror-curves.

### 1. Introduction

Mirror-curves originated from matting, plaiting, and basketry. They appear in arts of different cultures (as Celtic knots, Tamil threshold designs, Sona sand drawings...), as well as in works of Leonardo and Dürer. Gerdes recognized their deep connection with the mathematical algorithmic-based structures: knot mosaics, Lunda matrices, self-avoiding curves, and cell-automata [1, 2, 3, 4].

Mirror curves are constructed out of rectangular square grids, denoted by  $RG[p, q]$ , of size  $p, q$  ( $p, q \in N$ ). First we connect the midpoints of adjacent edges of  $RG[p, q]$  to obtain a 4-valent graph: every vertex of this graph is incident to four edges, called *steps*. Next, choose a starting point and traverse the curve so that we leave each vertex via the middle outgoing edge. If we return to the starting point, closing a path called a *component*, we choose a different one and repeat the process until every step is used exactly once. A *mirror-curve* in  $RG[p, q]$  grid is the set of all components. To obtain a knot or a link diagram from the mirror curve we introduce the “over-under” relation, turning each vertex to the crossing, i.e., we choose a pair of collinear steps (out of two) meeting at a vertex to be the overpass [5].

Mirror-curves can also be obtained from the following physical model: consider that the sides of our rectangular square grid  $RG[p, q]$  are made of mirrors, and that additional internal two-sided mirrors are placed between the square cells, coinciding with an edge, or perpendicular to it in its midpoint. If a ray of light is emitted from one edge-midpoint at an angle of  $45^\circ$ , it will eventually come back to its starting point, closing a component after series of reflections. If some steps remained untraced, repeat the whole procedure starting from a different point.

---

2010 *Mathematics Subject Classification*: 57M25, 57M27.

Partially supported by the Serbian Ministry of Science, Project 174012.

Through the rest of the paper the term “mirror-curve” will be used for a labeled mirror-curve. Hence, all crossings will be signed, where  $+1$  corresponds to positive, and  $-1$  to negative crossings.

**THEOREM 1.1.** [3] *The number of components of a knot or link  $L$  obtained from a rectangular grid  $\text{RG}[p, q]$  without internal mirrors is  $c(L) = \text{gcd}(p, q)$ .*

The web-Mathematica computations with mirror-curves are available at the address: <http://math.ict.edu.rs:8080/webMathematica/mirror/cont.htm>

Up to some point, the paper is an extended summary of the paper [6] by the authors together with collaborators, where it is shown that mirror-curve codes together with a set of appropriate equivalence moves capture all information about isotopy classes of knot and link diagrams, and that this theory is equivalent to the theory of mosaics by Kauffman and Lomonaco, and even more economical. Beyond summarizing the theory of mirror curves, we go further with presenting and discussing an interesting application of mirror-curves in obtaining knots and links in chiral nematic colloids.

## 2. Coding of mirror-curves

Mirror curve is constructed on a rectangular grid  $\text{RG}[p, q]$  with every internal edge labeled  $1$ ,  $-1$ ,  $2$ , and  $-2$ , where  $1$  and  $-1$  denote, respectively, a positive and negative crossing in the middle point of the edge (Fig. 1a), while  $2$  and  $-2$  denote a two-sided mirror incident with the edge, either collinear or perpendicular to it, containing the middle point of the edge. The code for the mirror curves is the matrix (list of lists), containing labels of internal edges corresponding to rows and columns of the  $\text{RG}[p, q]$ . For example, the code

$$Ul = \{ \{-2, -1, -1, 2\}, \{1, 2, -1, 1\}, \{2, 1, -1\}, \{1, -2, -1\}, \{1, -2, -1\} \}.$$

corresponds to the mirror curve (Fig. 1c) based on the labeled rectangular grid  $\text{RG}[3, 2]$  shown in Fig. 1b.

## 3. Reduction of mirror-curves

Labeled mirror curves represent knot and link (shortly  $KL$ ) diagrams. In this section we consider Reidemeister moves and their effects, expressed in the language of mirror-curves. The Reidemeister move  $RI$  is equivalent to replacing crossing by the mirror  $-2$  (i.e.,  $\pm 1 \rightarrow -2$ ) (Fig. 2a). Reidemeister move  $RII$  is the replacement of two neighboring crossings of the same sign by two perpendicular or collinear mirrors (Fig. 2b), and Reidemeister move  $RIII$  is illustrated in Fig. 2c. The reduction process we have described will not always result in the minimal rectangular grid for representing a given  $KL$  as a mirror-curve. Therefore we need so-called “all-over move” (Fig. 3b) reducing the size of the grid from  $\text{RG}[p, q]$  to  $\text{RG}[p - 1, q]$  while preserving the knot or link type. In the reduction process, sometimes it is useful to use topological intuition to simplify the reduction, such as the mirror-moves shown in Fig. 3a, where the mirror which is repositioned is shown by a dotted line. Notice that every unknot or unlink can be reduced to the code containing only labels  $2$  and  $-2$ . Minimal diagrams of mirror curves correspond to

the codes with the minimal number of  $\pm 1$  labels. Minimal mirror-curve codes of alternating knots and links contain either 1 or  $-1$ , but not both of them.

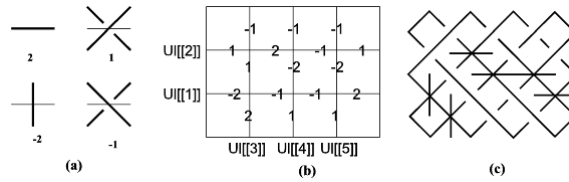


FIGURE 1. (a) Edge labeling; (b) labeled  $RG[3, 2]$ ; (c) the mirror-curve corresponding to the code  $UL$ .

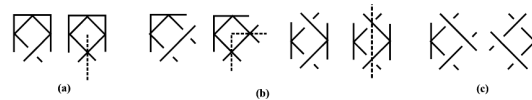


FIGURE 2. (a) Reidemeister move  $RI$ ; (b) Reidemeister move  $RII$ ; (c) Reidemeister move  $RIII$ , with additional mirrors in  $RI$  and  $RII$  denoted by dotted lines.

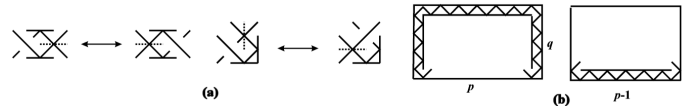


FIGURE 3. (a) Mirror move; (b) all-over move.

#### 4. Derivation of knots and links from mirror-curves

Another interesting open problem is which knots and links can be obtained from a rectangular grid  $RG[p, q]$  of a fixed size. To remove redundancies, we list each knot or link only once, associated only with the smallest rectangular grid from which it can be obtained. Knots and links are given by their classical notation and Conway symbols [5] from Rolfsen's tables [7]. Links with more than 9 crossings are given by Thistlethwaite's link notation, and links with  $n = 12$  crossings are given only by their Conway symbols.

Obviously, grid  $RG[1, 1]$  contains only the unknot, while from  $RG[2, 1]$  we can additionally derive the trivial two-component unlink. In general, every rectangular grid  $RG[p, 1]$  contains the trivial  $p$ -component unlink.

$RG[2, 2]$  without internal mirrors, taken as the alternating link, represents the link  $4_1^2$  (or its mirror image). It contains three different prime  $KL$ s: Hopf link 2 ( $2_1^2$ ), trefoil 3 ( $3_1$ ) and link 4 ( $4_1^2$ ). Hence, derived  $KL$ s can be treated as the states

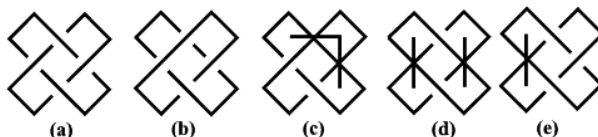


FIGURE 4. (a) Link 4 ( $4_1^2$ ); (b) non-minimal diagram of the Hopf link 2 ( $2_1^2$ ); (c,d) two minimal diagrams of the Hopf link; (e) minimal diagram of the trefoil knot 3 ( $3_1$ ).

of the link  $4_1^2$  obtained by substituting its crossings by elementary tangles 1,  $-1$ ,  $L_0$  and  $L_\infty$  (a “horizontal” and “vertical” smoothing) (Fig. 4).

From  $\text{RG}[3, 2]$  and its corresponding alternating knot  $3\ 1\ 3$  ( $7_4$ ) with the code  $\{\{1, 1, 1\}, \{1, 1\}, \{1, 1\}\}$ , we obtain the following prime  $KL$ s: knot  $4\ 2$  ( $6_1$ ) with the code  $\{\{1, 1, -1\}, \{1, 1\}, \{-1, -1\}\}$ , knot  $3\ 1\ 2$  ( $6_2$ ) with the code  $\{\{1, 1, 1\}, \{1, 1\}, \{-2, 1\}\}$ , link  $6$  ( $6_1^2$ ) with the code  $\{\{1, 2, 1\}, \{1, 1\}, \{1, 1\}\}$ , knot  $5$  ( $5_1$ ) with the code  $\{\{1, 2, 1\}, \{-2, 1\}, \{1, 1\}\}$ , knot  $3\ 2$  ( $5_2$ ) with the code  $\{\{1, 1, 1\}, \{1, 1\}, \{-2, -2\}\}$ , Whitehead link  $2\ 1\ 2$  ( $5_1^2$ ) with the code  $\{\{1, 1, 1\}, \{-2, 1\}, \{1, -2\}\}$ , and figure-eight knot  $2\ 2$  ( $4_1$ ) with the code  $\{\{-2, 1, 1\}, \{1, 1\}, \{-2, -2\}\}$ .

Alternating link  $3\ 1\ 2\ 1\ 3$  ( $L10a_{101}$  from Thistlethwaite’s tables) corresponds to the grid  $\text{RG}[4, 2]$ , from which we obtain the following prime  $KL$ s:  $5\ 1\ 3$  ( $9_5$ ),  $3\ 1\ 2\ 1\ 2$  ( $9_{20}$ ),  $4\ 1\ 1\ 3$  ( $9_5^2$ ),  $3\ 1\ 3\ 2$  ( $9_8^2$ ),  $3\ 1\ 1\ 1\ 3$  ( $9_9^2$ ),  $5\ 1\ 2$  ( $8_2$ ),  $4\ 1\ 3$  ( $8_4$ ),  $3\ 1\ 1\ 1\ 2$  ( $8_{13}$ ),  $8$  ( $8_1^2$ ),  $4\ 2\ 2$  ( $8_3^2$ ),  $3\ 2\ 3$  ( $8_4^2$ ),  $3\ 1\ 2\ 2$  ( $8_5^2$ ),  $2\ 4\ 2$  ( $8_6^2$ ),  $2\ 1\ 2\ 1\ 2$  ( $8_7^2$ ),  $7$  ( $7_1$ ),  $5\ 2$  ( $7_2$ ),  $2\ 2\ 1\ 2$  ( $7_6$ ),  $2\ 1\ 1\ 1\ 2$  ( $7_7$ ),  $4\ 1\ 2$  ( $7_1^2$ ),  $3\ 1\ 1\ 2$  ( $7_2^2$ ),  $2\ 3\ 2$  ( $7_3^2$ ),  $2\ 1\ 1\ 2$  ( $6_3$ ),  $3\ 3$  ( $6_2^2$ ), and  $2\ 2\ 2$  ( $6_3^2$ ).

**THEOREM 4.1.** [6] *All rational knots and links can be derived as mirror-curves from rectangular grids  $\text{RG}[p, 2]$  ( $p \geq 2$ ).*

From alternating link  $8^*2 : 2 : 2 : 2$  and  $\text{RG}[3, 3]$ , we derive the following prime  $KL$ s:  $(2, 2)$  ( $31, -31$ ),  $(-5\ 1, 2)$  ( $2, 2$ ),  $6^* - 2.2. - 2 : 4$ ,  $6^*3.2. - 3 : 2$ ,  $6^* - 3. - 3\ 0 :: -3\ 0$ ,  $2\ 1\ 2\ 1\ 1\ 1\ 2$  ( $10_{44}$ ),  $.4.2\ 0$  ( $10_{85}$ ),  $4\ 1\ 2\ 1\ 2$  ( $L10a_{99}$ ),  $.3 : 3\ 0$  ( $L10a_{140}$ ),  $6, 2, 2$  ( $L10a_{145}$ ),  $.2.3.2\ 0$  ( $L10a_{162}$ ),  $8^*2 :: 2$  ( $L10a_{163}$ ),  $2\ 0.2.2\ 0.2\ 0$  ( $L10a_{164}$ ),  $(2\ 1, -2\ 1)$  ( $2, 2$ ) ( $L10n_{73}$ ),  $(3\ 1, -2)$  ( $2, 2$ ) ( $L10n_{85}$ ),  $(2, 2)$  ( $4, -2$ ) ( $L10n_{86}$ ),  $4, 3\ 1, -2$  ( $L10n_{92}$ ),  $4, 4, -2$  ( $L10n_{93}$ ),  $2\ 0. - 2. - 2\ 0.2\ 0$  ( $L10n_{94}$ ),  $3\ 1, 3\ 1, -2$  ( $L10n_{95}$ ),  $4\ 1\ 2\ 2$  ( $9_{11}$ ),  $4\ 1\ 1\ 1\ 2$  ( $9_{14}$ ),  $2\ 1\ 3\ 1\ 2$  ( $9_{17}$ ),  $2\ 2\ 1\ 2\ 2$  ( $9_{23}$ ),  $2\ 1\ 2\ 1\ 1\ 2$  ( $9_{27}$ ),  $2\ 1\ 1\ 1\ 1\ 1\ 2$  ( $9_{31}$ ),  $6\ 1\ 2$  ( $9_1^2$ ),  $2\ 2\ 1\ 1\ 1\ 2$  ( $9_{12}^2$ ),  $5, 2, 2$  ( $9_{13}^2$ ),  $.4$  ( $9_{31}^2$ ),  $.3.2\ 0$  ( $9_{35}^2$ ),  $8^*2$  ( $9_{42}^2$ ),  $6\ 2$  ( $8_1$ ),  $3, 3, 2$  ( $8_5$ ),  $4\ 1\ 1\ 2$  ( $8_7$ ),  $2\ 3\ 1\ 2$  ( $8_8$ ),  $2\ 1, 3, 2$  ( $8_{10}$ )  $2\ 2\ 2\ 2$  ( $8_{12}$ ),  $2\ 2\ 1\ 1\ 2$  ( $8_{14}$ ),  $.2.2\ 0$  ( $8_{16}$ ),  $.2.2$  ( $8_{17}$ ),  $8^*$  ( $8_{18}$ ),  $2\ 1\ 2\ 1\ 2$  ( $8_7^2$ ),  $2\ 1\ 1\ 1\ 1\ 2$  ( $8_8^2$ ),  $4, 2, 2$  ( $8_1^3$ ),  $3\ 1, 2, 2$  ( $8_3^3$ ),  $(2, 2)$  ( $2, 2$ ) ( $8_4^3$ ),  $.3$  ( $8_5^3$ ),  $.2 : 2\ 0$  ( $8_6^3$ ),  $4, 2, -2$  ( $8_7^3$ ),  $3\ 1, 2, -2$  ( $8_8^3$ ),  $(2, 2)$  ( $2, -2$ ) ( $8_9^3$ ),  $(2, 2) - (2, 2)$  ( $8_{10}^3$ ),  $4\ 3$  ( $7_3$ ),  $3\ 2\ 2$  ( $7_5$ ),  $2, 2, 2+$  ( $7_1^2$ ),  $2\ 3\ 2$  ( $7_3^2$ ),  $3, 2, 2$  ( $7_4^2$ ),  $2\ 1, 2, 2$  ( $7_5^2$ ),  $.2$  ( $7_6^2$ ),  $2, 2, 2$  ( $6_1^3$ ),  $6^*$  ( $6_2^3$ ), and  $2, 2, -2$  ( $6_3^3$ ).

Mirror-curves are equivalent to link mosaics [8]: every link mosaic can be easily transformed into a mirror-curve and *vice versa* (Fig. 5). Kuriya [9] proved Lomonaco–Kauffman conjecture [8], showing that tame knots are equivalent to knot mosaics, hence also to mirror-curves, as well as to grid diagrams [10, 11].

This means that every  $KL$  can be represented as a mirror-curve placed in a RG of sufficiently large size.

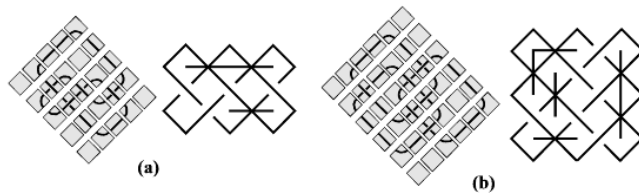


FIGURE 5. (a) Figure-eight knot and (b) Borromean rings from [8] transformed into mirror-curves.

### 5. Application of mirror curves

In [12], the authors used a restricted construction based on mirror curves in order to obtain different knots and links in chiral nematic colloids. They demonstrated the knotting of microscopic topological defect lines in chiral nematic liquid-crystal colloids into knots and links of arbitrary complexity by using laser tweezers as a micromanipulation tool. As the result they discerned almost 40 different knot and link types among  $3^9$  tangle combinations with minimum crossing numbers up to 10, and concluded that such a large diversity of topological objects suggests that it is possible to design any knot or link in a sufficiently large area (a rectangular square grid).



FIGURE 6. Restricted construction [12].

Analyzing their construction we conclude that on the left and right border of every array is placed a series of curls that can be eliminated by Reidemeister moves RI. All crossings corresponding to spheres are  $-1$  crossings, and the empty places (denoted by  $?$ , Fig. 6) can be substituted by a  $+1$  crossing, mirror 2, or mirror  $-2$  (“horizontal” or “vertical” smoothing). In the general construction, crossings  $+1$ ,  $-1$ , or mirrors 2,  $-2$  are permitted in every such empty position. Because of that restriction, the set of mirror curves obtained by this (restricted) construction is the subset of all mirror curves placed in rectangular grids. For the set of all mirror curves obtained by general construction it is proved that every knot or link can be modeled by some mirror curve placed in a sufficiently large area.

In order to check and extend the results obtained in [12], using the construction with the mentioned restriction, in the program “LinKnot” we succeeded to obtain all knots and links from the paper [12], including two more links,  $6_2^2 = 3\ 3$  and  $9_{49}^2 = 4, 3, -2$  that can be obtained from  $RG[4, 3]$ . Moreover, from larger rectangular grids we obtained more than 1000 different knots and links up to 12 crossings. Among them, we obtained all knots and links up to  $n = 8$  crossings, and all knots and links with  $n = 9$  crossings, except nine of them: knots  $9_{24}, 9_{34}, 9_{37}, 9_{40}$ , and two-component links  $9_{20}^2, 9_{23}^2, 9_{34}^2, 9_{42}^2$ . However, we are still not able to prove that all knots and links can be constructed by the restricted construction in a sufficiently large area, so we propose the question:

**Open problem.** Prove that all knots and links can be designed in a sufficiently large area by using the restricted construction.

### References

1. P. Gerdes, *Lunda Geometry—Designs, Polyominoes, Patterns, Symmetries*, Universidade Pedagógica Moçambique, Maputo, 1996.
2. P. Gerdes, *On mirror curves and Lunda designs*, *Computers&Graphics* **21:3**, (1997), 371–378.
3. P. Gerdes, *Geometry from Africa: Mathematical and Educational Explorations*, Mathematical Association of America, Washington, DC, 1999.
4. P. Gerdes, *Sona Geometry from Angola: mathematics of an African tradition*, Polimetrica, Milan, Italy, 2006.
5. S. V. Jablan, R. Sazdanović, *LinKnot- Knot Theory by Computer*, World Scientific, New Jersey, London, Singapore, 2007 (<http://math.ict.edu.rs/>).
6. S. Jablan, Lj. Radović, R. Sazdanović, A. Zeković, *Mirror-curves and knot mosaics*, *Comput. Math. Appl.* **64** (2012), 527–543 (see also arXiv:1106.3784v2).
7. D. Rolfsen, *Knots and Links*, Publish or Perish, 1976, (second edition, 1990; third edition, AMS Chelsea Publishing, 2003).
8. S. J. Lomonaco, L. H. Kauffman, *Quantum knots and mosaics*, *Quantum Inf. Process.* **7**(2008), 85–115, arXiv:quant-ph/0805.0339v1.
9. T. Kuriya, *On a Lomonaco-Kauffman conjecture*, arXiv:math.GT/0811.0710v3 (2008)
10. C. Manolescu, P. Ozsváth, Z. Szábo, D. Thurston, *On combinatorial link Floer homology*, arXiv:math.GT/0610559v2, (2007).
11. J. Baldwin, W. Gillam, *Computations of Heegaard–Floer knot homology*, arXiv:math.GT/0610167v3, (2007)
12. U. Tkalec, M. Ravnik, S. Čopar, S. Žumer, I. Mušević, *Reconfigurable knots and links in chiral nematic colloids*, *Science* **1**, July 2011, **333**, 6038, 62–65.

Department of Mathematics  
 Faculty of Mechanical Engineering  
 Niš  
 Serbia  
 ljradovic@gmail.com

Mathematical Institute  
 Knez Mihailova 36  
 B.O. Box 367  
 Belgrade  
 Serbia  
 sjablan@gmail.com